22nd IMEKO TC4 International Symposium & 20th International Workshop on ADC Modelling and Testing
SUPPORTING WORLD DEVELOPMENT THROUGH ELECTRICAL&ELECTRONIC MEASUREMENTS
IASI, ROMANIA, September 14-15, 2017

Accurate Amplitude Estimation of a Noisy Sine-wave via Interpolated DFT Algorithm

Daniel Belega[1], Dario Petri[2], Dominique Dallet[3]

[1]*Department of Measurements and Optical Electronics, University Politehnica Timisoara, Bv. V. Parvan, Nr. 2, 300223, Timisoara, Romania, email: daniel.belega@upt.ro*
[2]*Department of Industrial Engineering, University of Trento, Via Sommarive, 9, 38123, Trento, Italy, email: dario.petri@unitn.it*
[3]*IMS Laboratory, Bordeaux INP, University of Bordeaux, CNRS UMR5218, 351 Cours de la Libération, Bâtiment A31, 33405, Talence Cedex, France, email: dominique.dallet@ims-bordeaux.fr*

***Abstract* – This paper analyses Mean Square Error (MSE) of a noisy sine-wave amplitude estimator based on the Discrete-Time Fourier Transform (DTFT) evaluated at the signal frequency estimated by the classical Interpolated Discrete Fourier Transform (IpDFT) algorithm. In order to reduce the contribution of the spectral image component on the returned estimates, the sine-wave is weighted by a Maximum Sidelobe Decay (MSD) window. An analytical expression for the estimator MSE is derived. For given Signal-to-Noise Ratio (*SNR*) and number of processed samples, that expression allows us to derive the minimum number of acquired sine-wave cycles ensuring that the detrimental contribution of the image component on the estimation accuracy is negligible as compared with the effect of wideband noise. In such condition, both computer simulations and experimental results show that the analysed DTFT-based estimator outperforms the classical DFT-based estimator.**

Keywords* – *amplitude estimation, Discrete-Time Fourier Transform (DTFT), error and statistical analysis, windowing

I. INTRODUCTION

In many engineering fields, such as communications, radar, power systems, vibration analysis, and instrumentation, sine-wave parameters often need to be accurately estimated in real-time. The Interpolated Discrete Fourier Transform (IpDFT) algorithm is widely used to this purpose [1-6]. Indeed, when non-coherent sampling occurs, DFT-based frequency estimates are affected by the so-called "picket-fence" and spectral leakage errors. The former error is reduced by estimating the inter-bin frequency location by interpolating the two largest DFT spectral samples of the analysed signal. Spectral leakage is reduced by weighting the analysed signal by means of a suitable window. Cosine-class windows are often employed. In particular, the Maximum Sidelobe Decay (MSD) windows [7] are commonly used since signal frequency can be estimated by simple expressions [1, 4, 5]. In the classical IpDFT approach the sine-wave amplitude and phase are then estimated considering the estimated frequency and the largest DFT spectral sample, that is the one at the normalized frequency equal to the integer part of the number of acquired sine-wave cycles. Recently, it has been shown that the contribution of wideband noise on the estimation of complex-valued sine-wave amplitude is minimized when considering the Discrete-Time Fourier Transform (DTFT) spectral sample at the estimated normalized signal frequency [8]. However, the accuracy of that DTFT-based amplitude estimator when applied to a real-valued sine-wave has not been analysed yet. The aim of this paper is to derive an expression for that estimator Mean Square Error (MSE) considering the contribution of both the signal image component and wideband noise. For given Signal-to-Noise Ratio (*SNR*) and number of processed samples, that expression allows us to determine the minimum number of acquired sine-wave cycles ensuring that the effect of the image component on the estimation accuracy is negligible as compared with the influence of wideband noise. Furthermore, the accuracy of the DTFT-based and the DFT-based amplitude estimators are compared each other using both simulation and experimental data.

II. DTFT-BASED AMPLITUDE ESTIMATOR

The analysed discrete-time noisy sine-wave is modelled as:

$$y(m) = A\sin(2\pi fm + \phi) + e(m),\ m = 0,1,\ldots,M-1 \quad (1)$$

where A, f, and ϕ are the amplitude, the normalized frequency, and the initial phase of the sine-wave, $e(\cdot)$ is a white Gaussian noise with zero mean and variance σ^2, and M is the number of acquired samples. The normalized frequency, defined as the ratio between the continuous-time

sine-wave frequency f_{in} and the sampling rate f_s, can be expressed as:

$$f = \frac{f_{in}}{f_s} = \frac{\kappa}{M} = \frac{l+\varepsilon}{M}, \quad (2)$$

where $\nu = l + \varepsilon$ is the number of acquired sine-wave cycles, l is its integer part and ε ($-0.5 \le \varepsilon < 0.5$) is the inter-bin frequency location. In most practical situations non-coherent sampling occurs (i.e. $\varepsilon \neq 0$), so that the "picket-fence" and the spectral leakage phenomena arise. Spectral leakage can be reduce by weighting the analysed signal using a suitable window function $w(\cdot)$. The DTFT of the windowed signal $y_w(m) = y(m) \cdot w(m)$ is given by [4]:

$$Y_w(\lambda) = \frac{A}{2j}\left[W(\lambda-\nu)e^{j\phi} - W(\lambda+\nu)e^{-j\phi}\right] + E_w(\lambda), \quad (3)$$

where $W(\cdot)$ is the DTFT of the used window $w(\cdot)$ and $E_w(\cdot)$ is the DTFT of the weighted noise $e_w(m) = e(m) \cdot w(m)$.

When the H-term MSD window is used, for $|\lambda| << M$, we have [5]:

$$W(\lambda) = \frac{M \sin(\pi\lambda)}{2^{2H-2}\pi\lambda} \frac{(2H-2)!}{\prod_{h=1}^{H-1}\left(h^2-\lambda^2\right)} e^{-j\pi\lambda}. \quad (4)$$

In that case, the fractional frequency estimator $\hat{\varepsilon}$ provided by the IpDFT algorithm is [5]:

$$\hat{\varepsilon} = \frac{(H+i-1)\alpha - H + i}{\alpha + 1}, \quad (5)$$

where $\alpha \overset{\Delta}{=} |Y_w(l+i)| / |Y_w(l-1+i)|$, in which $i = 0$ if $|Y_w(l-1)| \ge |Y_w(l+1)|$ and $i = 1$ if $|Y_w(l-1)| < |Y_w(l+1)|$.

Assuming that l is exactly determined [4], the estimator of the number of acquired sine-wave cycles is $\hat{\kappa} = l + \hat{\varepsilon}$ and the related DTFT-based amplitude estimator is given by [8]:

$$\hat{A} = \frac{2|Y_w(\hat{\kappa})|}{W(0)}. \quad (6)$$

III. MSE OF THE DTFT-BASED AMPLITUDE ESTIMATOR

The amplitude estimation error due to the spectral interference from the fundamental image component can be expressed as (see Appendix):

$$\Delta_{A_{si}} \overset{\Delta}{=} \hat{A} - A \cong p\Delta_{A_{si,\max}} \cos(2\pi\varepsilon + 2\phi), \quad (7)$$

where

$$\Delta_{A_{si},\max} = A\frac{|W(2\kappa)|}{W(0)}, \quad (8)$$

and $p = (-1)^H \mathrm{sgn}(\varepsilon)$, in which $\mathrm{sgn}(\cdot)$ is the sign function.

Referring to the behaviour of the window DTFT (4), when at least $(H+1)/2$ sine-wave cycles are acquired, from (7) and (8) it follows that:

$\Delta_{A_{si}}$ is null when $\varepsilon = 0$ (i.e. coherent sampling occurs), or $\varepsilon = -0.5$;

$\Delta_{A_{si},\max}$ is maximum when $\varepsilon = -0.25$;

$\Delta_{A_{si},\max}$ decreases as κ and/or H increases.

However, when analysing a noisy sine-wave, the DTFT-based amplitude estimator is affected also by wideband noise. Since its effect can be considered statistically independent of the contribution of the spectral image component, the amplitude estimator MSE is expressed by:

$$MSE[\hat{A}] = E[\Delta^2_{A_{si}}] + E[\Delta^2_{A_n}], \quad (9)$$

where E[·] denotes the expectation operator and Δ_{A_n} represents the estimation error due to wideband noise.

Assuming that the sine-wave phases ϕ related to subsequent acquisitions vary at random in the range $[0, 2\pi)$ rad (as it happens in practice in the case of non-coherent sampling), from (7) it follows that:

$$E[\Delta^2_{A_{si}}] \cong 0.5\Delta^2_{A_{si,\max}}. \quad (10)$$

Moreover [8]:

$$E[\Delta^2_{A_n}] \cong \sigma^2_{\hat{A}} \cong \frac{2}{M} ENBW\sigma^2 \cong ENBW(\sigma^2_A)_{CR}, \quad (11)$$

in which $ENBW$ is the window Equivalent Noise BandWidth [9] and $(\sigma^2_A)_{CR} \cong 2\sigma^2 / M$ is the Cramèr-Rao Lower Bound (CRLB) for unbiased amplitude estimators [4]. For the H-term MSD window we have $ENBW = C^{2H-2}_{4H-4} / (C^{H-1}_{2H-2})^2$, where $C^q_n = n!/((n-q)!q!)$ [5].

By replacing (10) and (11) in (9) we have:

$$MSE[\hat{A}] \cong 0.5\Delta^2_{A_{si,\max}} + \frac{2}{M} ENBW\sigma^2. \quad (12)$$

When a sufficiently high number of cycles κ is observed, the contribution on the estimated amplitude of the interference from the fundamental image component is negligible as compared with the effect of wideband noise. Thus, the statistical efficiency of the DTFT-based estimator becomes $(\sigma^2_A)_{CR} / \sigma^2_{\hat{A}} \cong 1/ENBW$, which decreases as

ENBW (or equivalently *H*) increases, that is with more tapered windows. If the two-term MSD window (or Hann window) is used, we have *ENBW* = 1.5 and $(\sigma_A^2)_{CR} / \sigma_{\hat{A}}^2 \cong 0.67$.

IV. CONSTRAINT ENSURING THAT THE IMAGE COMPONENT CONTRIBUTION ON THE DTFT-BASED AMPLITUDE ESTIMATOR IS NEGLIGIBLE

It is of interest to determine the minimum number of signal cycles l_{min} that ensures that the contribution on the estimated amplitude of the fundamental image component is negligible as compared with the effect of wideband noise. To this aim, since the worst case interference from the fundamental image component occurs at ε = -0.25, we consider the following inequality:

$$E[\Delta_{A_n}^2] \geq 10 E[\Delta_{A_{si}}^2]\Big|_{\varepsilon=-0.25}. \qquad (13)$$

For given values of *SNR* and number of signal samples *M*, using (4), (8), (10), and (11), expression (13) provides:

$$SNR\ (dB) = 20\log 10\left(\frac{W(0)}{|W(2l_{\min} - 0.5)|}\sqrt{\frac{ENBW}{5M}}\right). \qquad (14)$$

This expression is depicted in Fig. 1 for the Hann window, *M* = 512 and 4096 samples.

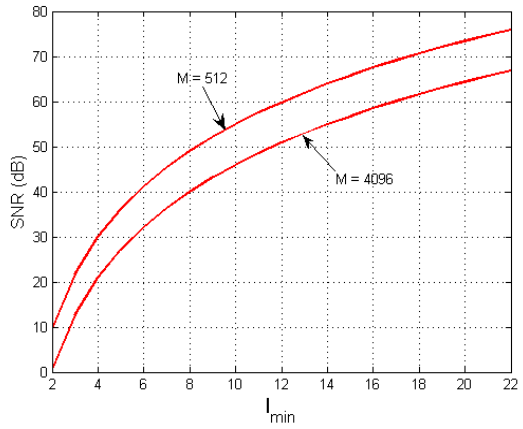

Fig. 1. Theoretical SNR versus l_{min} returned by (14) when the Hann window is adopted. M = 512 and 4096 samples

It can be seen that l_{min} increases as *M* increases since the MSE contribution due to wideband noise is inversely proportional to that parameter. It is also worth noticing that, when $l_{min} \geq 10$ the relationship (14) is almost linear. Indeed, the envelope of the sidelobes of the Hann window spectrum is almost proportional to the square value of the sine-wave normalized frequency.

V. COMPUTER SIMULATIONS AND EXPERIMENTAL RESULTS

In this Section the accuracies of expressions (7) and (12) are verified through computer simulations. Also, the accuracies of the DTFT-based and the DFT-based amplitude estimators are compared each other by means of both computer simulations and experimental results [1, 4, 5].

The Hann window is adopted. Moreover the sine-wave amplitude and the number of processed samples are *A* = 2 and *M* = 512, respectively. When performing statistical analysis, 1000 runs are considered by varying the sine-wave phase ϕ at random in the range [0, 2π) rad.

Fig. 2 shows the amplitude estimation errors $\Delta_{A_{si}}$ due to the fundamental image component as a function of the sine-wave phase ϕ when κ = 2.75 cycles and κ = 5.25 cycles, respectively. The results returned by both simulations and (7) are reported. The phase ϕ is varied with a step of π/50 rad.

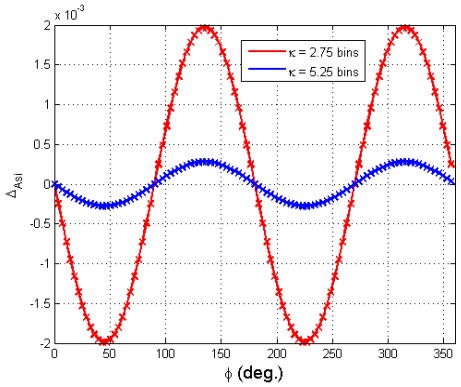

Fig. 2. Amplitude estimation error $\Delta_{A_{si}}$ due to the fundamental image component versus the sine-wave phase ϕ when κ = 2.75 and κ = 5.25 cycles. Simulation results (stars) and theoretical results (continuous line)

As we can see, there is a very good agreement between the theoretical and the simulation results. Also, the errors $\Delta_{A_{si}}$ decreases as κ increases, as expected.

Fig. 3 shows the simulation results and the theoretical values returned by (8) for the maximum amplitude estimation error $\Delta_{A_{si},\max}$ as a function of the number of observed sine-wave cycles κ. Moreover, the envelope of such error, which is reached for ε = -0.25, is also shown.

As we can see, the simulation and the theoretical results are very close each other.

Fig. 4 shows the simulated MSEs for both the classical DFT-based and the DTFT-based amplitude estimators as a function of the number of observed sine-wave cycles κ when *SNR* = 25 dB (Fig. 3a) and *SNR* = 50 dB (Fig. 3b). The theoretical MSE of the DTFT-based amplitude estimator returned by (12) and the related unbiased CRLB are also shown in the figure.

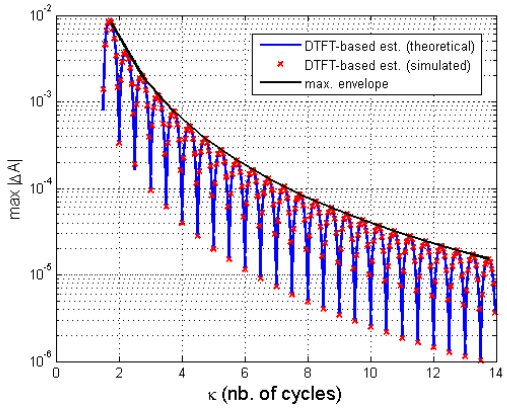

Fig. 3. Maximum of the amplitude estimation error $\Delta_{A_{si},\max}$ due to the spectral image component versus the number of acquired sine-wave cycles κ. Simulation results (stars) and theoretical results (continuous line). The envelope of the theoretical results is also shown

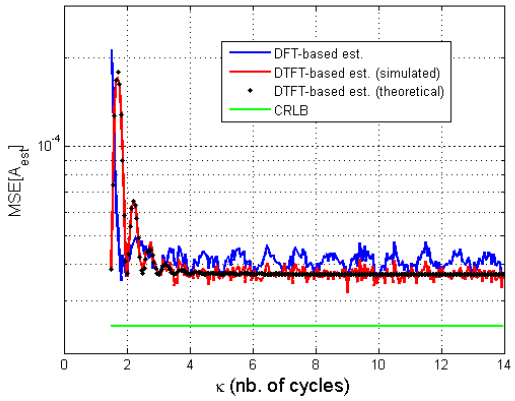

(a)

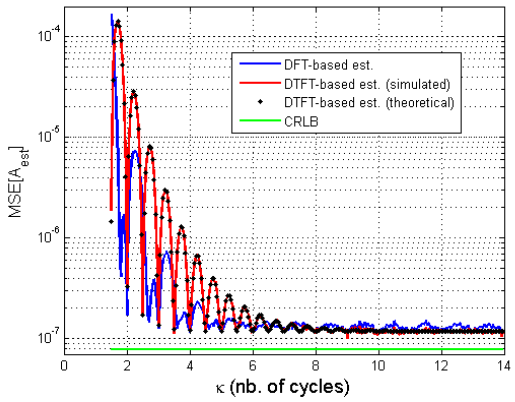

(b)

Fig. 4. MSE of the DFT-based and the DTFT-based amplitude estimators versus the number of acquired sine-wave cycles κ when SNR = 25 dB (a) and SNR = 50 dB (b). Theoretical MSE (12) (continuous line) and simulation results (dots). The related CRLB is also shown

As it can be seen, for small values of κ, when the contribution of the fundamental image component dominates, the DFT-based amplitude estimator outperforms the DTFT-based one. Conversely, when κ is high, the contribution of wideband noise dominates, and the opposite behaviour occurs. It is worth noticing that (14) returns l_{min} = 3 and l_{min} = 8 when *SNR* = 25 dB and 50 dB, respectively. These values well agree with the behaviours shown in Fig. 3. Thus, when $l \geq l_{min}$ the DTFT-based amplitude estimator outperforms the DFT-based one since the former algorithm minimizes the contribution of wideband noise on the returned estimates. Also, Fig. 4 shows that the simulation results related to the DTFT-based amplitude estimator fully agree with the theoretical results.

The theoretical analysis reported above was verified also by experiments. Sine-waves were generated by using an Agilent 33220A signal generator and then acquired by means of an NI6023 acquisition board with sampling rate f_s = 100 kHz. Their amplitude was A = 2 V, while the frequencies were varied in the ranges [500, 680] Hz and [3230, 3410] Hz, respectively, with a step of 20 Hz. For each frequency value 1000 runs of M = 512 samples each were acquired. Consequently, the number of acquired sine-wave cycles κ spanned the ranges (2.5, 3.5) and (16.5, 17.5), respectively. This quantity was estimated as the average of the values returned by the IpDFT algorithm. The *SNR* value estimated by the four-parameter sine-fit algorithm [10] was about 55 dB. The variances of both the DFT-based and the DTFT-based amplitude estimators are shown in Fig. 5 as a function of the number of sine-wave cycles κ.

This figure shows that the DFT-based estimator outperforms the DTFT-based one when $2.5 < \kappa < 3.5$ cycles, while the opposite occurs when $16.5 < \kappa < 17.5$ cycles. Indeed, in the former case the contribution of the spectral image component dominates estimation uncertainty, while in the latter case the contribution of wideband noise prevails. These results agree with theory since, when *SNR* = 55 dB, Fig. 1 shows that the DTFT-based algorithm provides very accurate amplitude estimates for $l \geq 10$.

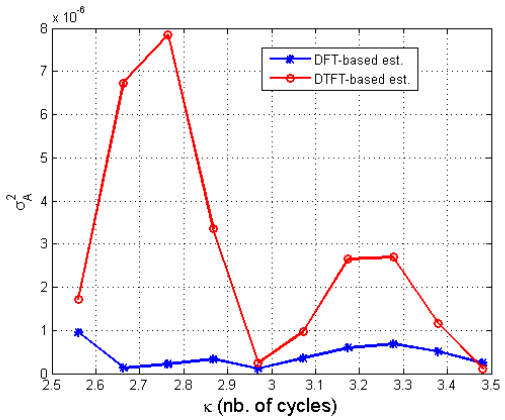

(a)

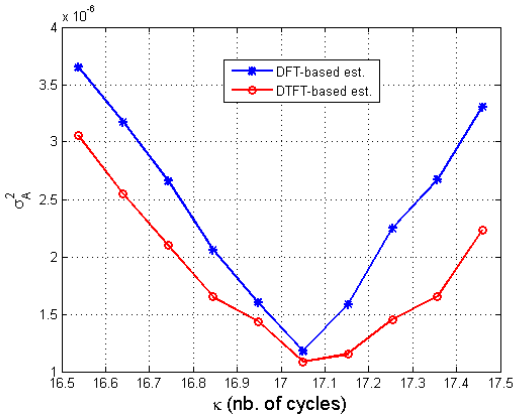

(b)

Fig. 5. Experimental results: variances of the DFT-based and the DTFT-based amplitude estimators versus the number of acquired sine-wave cycles κ. Sine-wave frequencies in the ranges [500, 680] Hz (a) and [3230, 3410] Hz (b), respectively

VI. CONCLUSIONS

In this paper the accuracy of the DTFT-based amplitude estimator proposed in [8] has been analysed in the case of noisy real-valued sine-waves. An analytical expression for the estimator MSE has been derived. For given *SNR* and number of processed samples, that expression allows us to derive the minimum number of acquired sine-wave cycles ensuring that the contribution on the estimation accuracy of the spectral image component is negligible as compared to the effect of wideband noise. When that constraint is satisfied both computer simulations and experimental results show that the DTFT-based amplitude estimator outperforms the classical DFT-based amplitude estimator.

APPENDIX

Derivation of the expression for the amplitude estimation error

By neglecting the contribution of wideband noise, since $\Delta\varepsilon = \hat{\varepsilon} - \varepsilon \cong 0$, we have:

$$Y_w(l+\hat{\varepsilon}) \cong \frac{A}{2j}W(0)e^{j\phi} - \frac{A}{2j}W(2l+2\varepsilon)e^{-j\phi}, \quad \text{(A.1)}$$

Using (4) we have:

$$Y_w(l+\hat{\varepsilon}) \cong \frac{A}{2j}W(0)e^{j\phi} + \frac{A}{2j}p\left|W(2l+2\varepsilon)\right|e^{-j(\phi+2\pi\varepsilon)}, \quad \text{(A.2)}$$

where $p \overset{\Delta}{=} (-1)^H \operatorname{sgn}(\varepsilon)$, in which sgn(·) is the sign function.

From (A.2), observing that $W(0) >> |W(2l + 2\varepsilon)|$, after some algebra it follows:

$$\left|Y_w(l+\hat{\varepsilon})\right|^2 \cong \frac{A^2}{4}W^2(0) \times \left[1 + 2p\frac{|W(2l+2\varepsilon)|}{W(0)}\cos(2\phi+2\pi\varepsilon)\right], \quad \text{(A.3)}$$

Using the approximation $\sqrt{1+x} \cong 1 + x/2$, when $|x| << 1$, we have:

$$\left|Y_w(l+\hat{\varepsilon})\right| \cong \frac{A}{2}\left[W(0) + p|W(2l+2\varepsilon)|\cos(2\phi+2\pi\varepsilon)\right]. \quad \text{(A.4)}$$

By replacing (A.4) in (6) we obtain:

$$\hat{A} \cong A + pA\frac{|W(2l+2\varepsilon)|}{W(0)}\cos(2\phi+2\pi\varepsilon). \quad \text{(A.5)}$$

From (A.5) the expression (7) for the amplitude estimation error $\Delta_{A_{si}}$ due to the interference from the spectral image component is finally obtained.

REFERENCES

[1] Rife, D.C, Vincent, G.A., *Use of the discrete Fourier transform in the measurement of frequencies and levels of tones*, Bell Syst. Tech. J., vol. 49, pp. 197-228, 1970.

[2] Grandke, T., *Interpolation algorithms for discrete Fourier transforms of weighted signals*, IEEE Trans. Instrum. Meas., vol. 32, no. 2, pp. 350 – 355, 1983.

[3] Quinn, B.G., *Estimation of frequency, amplitude, and phase from the DFT of a time series*, IEEE Trans. Signal Process., vol. 45, no. 3, pp. 814-817, 1997.

[4] Offelli, C., Petri, D., *The influence of windowing on the accuracy of multifrequency signal parameter estimation*, IEEE Trans. Instr. Meas., vol. 41, no. 2, pp. 256-261, 1992.

[5] Belega, D., Dallet, D., *Multifrequency signal analysis by interpolated DFT method with maximum sidelobe decay windows*, Measurement, vol. 42, no. 3, pp. 420-426, 2009.

[6] Aboutanios, E., Mulgrew, B., *Iterative frequency estimation by interpolation on Fourier coefficients*, IEEE Trans. Signal Process., vol. 53, no. 4, pp. 1237-1241, 2005.

[7] Nuttall, A.H., *Some windows with very good sidelobe behavior*, IEEE Trans. Acoust. Speech Signal Process. ASSP-29, vol. 1, pp. 84–91, 1981.

[8] Belega, D., Petri, D., Dallet, D., *Accuracy analysis of complex sinusoid amplitude and phase estimation by means of the discrete-time Fourier transform algorithm*, Digital Signal Process, vol. 59, pp. 9-18, 2016.

[9] Harris, F.J., *On the use of windows for harmonic analysis with the discrete Fourier transform*, Proceedings of the IEEE, vol. 66, no. 1, pp. 51–83, 1978.

[10] Standard IEEE 1057-2007, IEEE Standard for Digitizing Waveform Recorders, 2007.